Journal of Bioenergetics and Biomembranes, Vol. 32, No. 5, 2000

Inhibitory Mg-ADP–Fluoroaluminate Complexes Bound to Catalytic Sites of F_1-ATPases: Are They Ground-State or Transition-State Analogs?

William S. Allison,[1,2] Huimiao Ren,[1] and Chao Dou[1]

Schemes are proposed for coupling sequential opening and closing the three catalytic sites of F_1 to rotation of the γ subunit during ATP synthesis and hydrolysis catalyzed by the F_oF_1-ATP synthase. A prominent feature of the proposed mechanisms is that the transition state during ATP synthesis is formed when a catalytic site is in the process of closing and that the transition state during ATP hydrolysis is formed when a catalytic site is in the process of opening. The unusual kinetics of formation of Mg-ADP–fluoroaluminate complexes in one or two catalytic sites of nucleotide-depleted MF_1 and wild-type and mutant $\alpha_3\beta_3\gamma$ subcomplexes of TF_1 are also reviewed. From these considerations, it is concluded that Mg-ADP–fluoroaluminate complexes formed at catalytic sites of isolated F_1-ATPases or F_1 in membrane-bound F_oF_1 are ground-state analogs.

KEY WORDS: F_1-ATPase; transition-state analog; ground-state analog; rotational catalysis.

INTRODUCTION

The ATP synthases found in energy-transducing membranes couple translocation of protons or sodium ions to the condensation of ADP with P_i to form ATP. The enzymes are comprised of an integral membrane protein complex F_o that mediates ion translocation and a peripheral membrane complex F_1 that contains the catalytic sites for the condensation reaction. F_1 is connected to F_o by two narrow stalks. When removed from the membrane in soluble form, F_1 is an ATPase made up of five different subunits in $\alpha_3\beta_3\gamma\delta\varepsilon$ stoichiometry. In addition to its three catalytic sites, F_1 contains three additional nucleotide binding sites that are called noncatalytic sites.

In the crystal structure of the bovine heart mitochondrial F_1-ATPase (MF_1) solved by Abrahams *et al*. (1994), the α and β subunits are elongated and arranged alternately in an hexameric configuration. The cavity of the $(\alpha\beta)_3$ hexamer is filled with two α helices arising from the amino- and carboxyl-termini of the γ subunit, which are partly in the form of an antiparallel coiled-coil. The coiled-coil is asymmetrically arranged within the central cavity. Whereas all three noncatalytic sites, located at α/β interfaces, are homogeneously liganded with Mg-AMP–PNP, the three catalytic sites, located at different α/β interfaces, are heterogeneously liganded. The catalytic site at the α_{TP}/β_{TP} interface contains bound Mg-AMP–PNP, the catalytic site at the α_{DP}/β_{DP} interface contains bound Mg-ADP, and the third catalytic site at the α_E/β_E interface is empty. The conformation of β_E differs considerably from the nearly common conformation of β_{TP} and β_{DP}. Compared to β_{TP} and β_{DP}, the α-helical carboxyl-terminal domain of β_E is twisted away from the nucleotide-binding domain. The overall conformation of β_E is open, whereas the overall conformations of β_{TP} and β_{DP} are closed.

It was immediately recognized that the crystal structure of MF_1 is consistent with important predictions of the binding-change model proposed by Boyer in the late 1970s for ATP hydrolysis catalyzed by F_1 (Boyer, 1993, 2000). The binding-change model predicts that the three catalytic sites of F_1 act sequentially to promote rotation of single-copy subunits (γ and ε) with respect to the hexomeric ring, made up of the three α and three β subunits. This prediction was rapidly validated by experiments that

[1] Department of Chemistry and Biochemistry, University of California at San Diego, La Jolla, California 92093-0506.
[2] To whom all correspondence should be addressed.

0145-479X/00/1000-0531$18.00/0

were designed on the basis of the crystal structure (Duncan *et al*., 1995; Sabbert *et al*., 1996; Noji *et al*., 1997; Yasuda *et al*., 1998). In the most elegant of these, a fluorescently labeled actin filament was attached to that part of the γ subunit that is outside the central cavity of the $\alpha_3\beta_3\gamma$ subcomplex of TF_1 (Noji *et al*., 1997; Yasuda *et al*., 1998). When Mg-ATP was added to the engineered, immobilized subcomplex, the actin filament rotated counter clockwise when viewed through a microscope. Equation (1) provides the minimal description of the hydrolytic process where ↺ represents counter clockwise rotation of the γ subunit.

$$ATP^{-4} + H_2O \rightarrow ADP^{-3} + H_2PO_4^- + \circlearrowleft \qquad (1)$$

By inference, ion translocation through F_o is thought to drive clockwise rotation of the γ subunit during ATP synthesis by the F_oF_1 complex. Equation 2 represents the minimal description of energy-dependent condensation of ADP with P_i catalyzed by the intact ATP synthase, where ↻ represents clockwise rotation of the γ subunit.

$$ADP^{-3} + H_2PO_4^- + \circlearrowright \rightarrow ATP^{-4} + H_2O \qquad (2)$$

ATP hydrolysis by the intact synthase coupled to clockwise rotation of the γ subunit is thought to drive ion translocation in the opposite direction through F_o. For recent reviews on coupling rotational catalysis to ion translocation see Fillingame (2000) and Groth (2000).

MODELS FOR COUPLING CATALYSIS BY F_1 TO SEQUENTIAL OPENING AND CLOSING OF CATALYTIC SITES

Table I illustrates the magnitude of the conformational change that occurs during interconversion of the open and closed forms of catalytic sites. Distances between functional groups of amino acid side chains at the α_{TP}/β_{TP} and α_{DP}/β_{DP} interfaces and the anionic oxygens of bound nucleotides and bound Mg^{2+} ions in the crystal structure of MF_1 are summarized in the table. Distances between pairs of the functional side chains in the three catalytic sites in the crystal structure are also compared. Amino acid side chains that interact with either the anionic oxygens of bound nucleotides or the Mg^{2+} ion in catalytic sites at the α_{TP}/β_{TP} and α_{DP}/β_{DP} interfaces are arranged very differently in the empty catalytic site (Allison, 1998; Ren and Allison, 2000b). For instance, the side chain hydroxyl group of βThr163 is directly coordinated to the Mg^{2+} ions in the catalytic sites at the α_{TP}/β_{TP} and α_{DP}/β_{DP} interface, whereas it is hydrogen bonded to the carboxylate of βGlu199 in the empty catalytic site.

Sequential hydrolysis of ATP at the three catalytic sites of F_1 coupled to rotation of the γ subunit is a highly cooperative process (Weber and Senior, 1997; Omote and Futai, 1998; Ren and Allison, 2000). ATP hydrolysis proceeds with long-distance, positive cooperative interactions between catalytic sites. Long-distance interactions between catalytic sites and the carboxyl-terminal α-helical domains of β subunits also occur. Basic features of the coupling mechanism include: (1) rapid rates of ATP hydrolysis are only attained when all three catalytic sites are saturated (Weber *et al*., 1993); and (2) only two β subunits can exist in the closed conformation simultaneously (Tsunoda *et al*., 1999). By correlating catalytic site occupancy with the rate of ATP hydrolysis using the βTyr345 Trp mutant of *E. coli* F_1, Weber *et al*. (1993) demonstrated that rapid rates of ATP hydrolysis are not observed until all three catalytic sites are saturated. Tsunoda *et al*. (1999) recognized that the Ile390 residues in β_{TP} and β_{DP} are in contact in the crystal structure of MF_1. Using this observation as a clue, they employed a combination of computer modeling and mutagenesis to demonstrate: (1) β subunits are converted from open to closed conformations when they bind Mg-ADP or Mg-ATP to catalytic sites; and (2) three β subunits cannot exist in closed conformations simultaneously. It was also found that cross links can only form within two β subunits when the $\alpha_3(\beta$D315C/R337 $C)_3\gamma$ double-mutant subcomplex of TF_1 is treated with oxidants (Ren *et al*., 1999). This also demonstrates that only two β subunits can exist in closed conformations simultaneously. (To avoid confusion, residue numbers of MF_1 only are used throughout this review.)

Figure 1 includes three different views of a limited section of the crystal structure of MF_1 that illustrate the relative positions of residue Ile390 within residues 380–400 of the three β subunits relative to segments of the γ subunit. The portion of the γ subunit that is illustrated in *gray* represents a segment of the coiled-coil (residues 6-39 and

Table I. Interaction Distances between Bound Nucleotides and Functional Groups and between Functional Groups at the Three Catalytic Sites in the Crystal Structure of MF_1[a]

Interaction	α_E/β_E	α_{DP}/β_{DP}	α_{TP}/β_{TP}
βK162N_ε-$O_\delta\beta$D256	2.7 Å	6.8 Å	6.7 Å
βT163O_γ-$O_\varepsilon\beta$E199	2.9	11.4	11.4
αR373NH-$O_\alpha\alpha$D347	3.0	6.5	6.4
αR373NH-$O_{\beta,\gamma}$AD(T)P		2.3	3.1
βR189NH-$O_{\beta,\gamma}$AD(T)P		5.4	3.0
βK162N_ε-$O_{\beta,\gamma}$AD(T)P		3.3	4.1
βE188O-$O_{\beta,\gamma}$AD(T)P		5.9	3.7
βE192O_ε-Mg^{2+}		4.4	4.0
βD256O_δ-Mg^{2+}		4.1	3.9
βE188O_ε-Mg^{2+}		5.1	3.6
βT163O_γ-Mg^{2+}		2.2	2.2

[a] Abrahams *et al*., 1994.

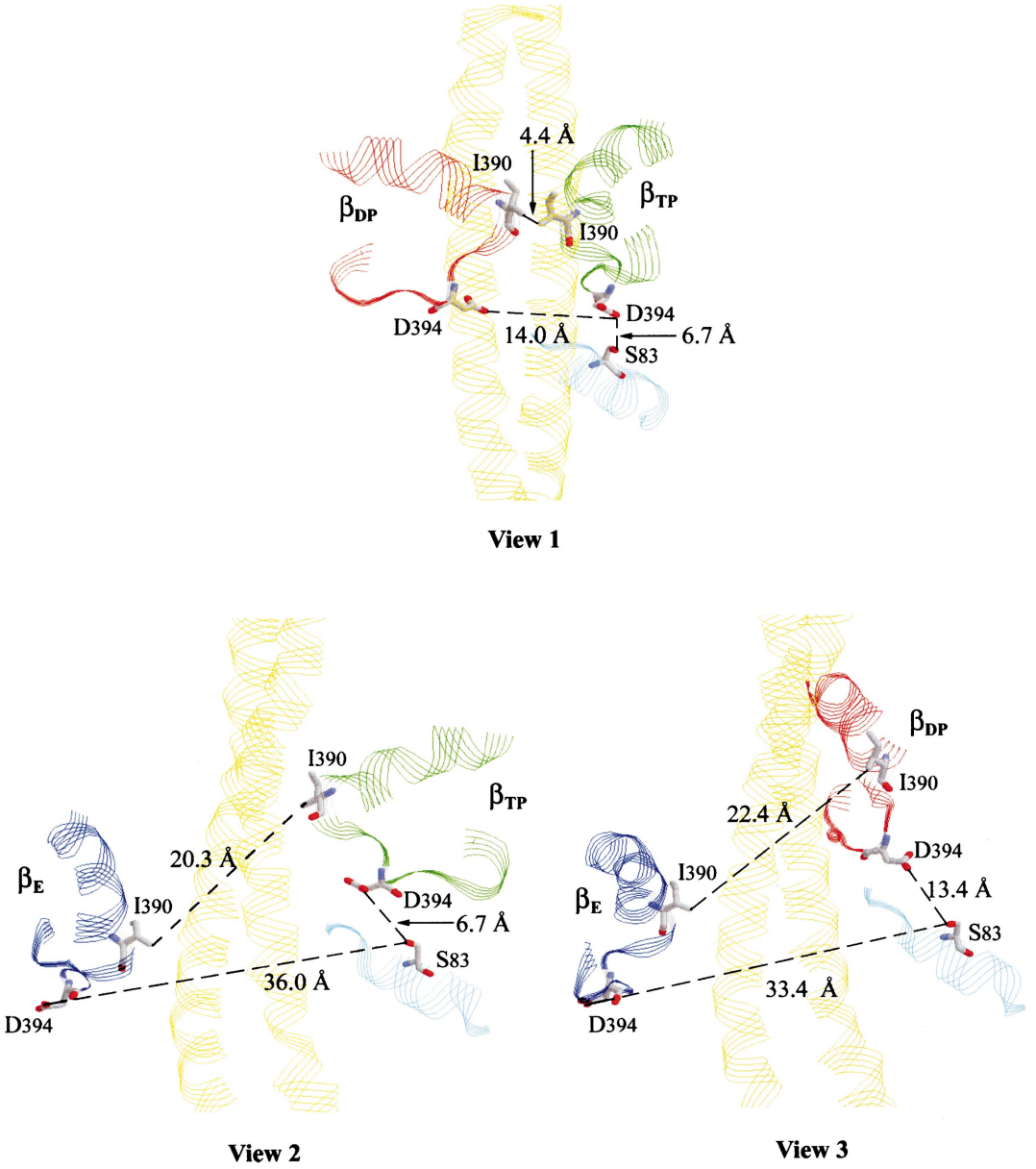

Fig. 1. Three views of a segment of the three β subunits in F_1 that illustrate the relative positions of Ile390 and Asp394 in β_E, β_{TP}, and β_{DP}. The three views also illustrate the position of γSer83 relative to Asp394 in the three β subunits in the crystal structure of MF_1. This figure was constructed from the coordinates of MF_1 (Abrahams *et al*., 1994) using the software program Rasmol provided by R. Sayle (Glaxo Wellcome Research and Development, Greenford, UK).

residues 217–246). The α-helical spur of the γ subunit containing residues 73–90 is *also* shown in *gray*. View 1 shows that the distance between the side chains of the two Ile390 residues in β_{DP} and β_{TP} in the crystal structure is only 4.4 Å. In contrast, the side chains of the Ile390 residues in β_E and β_{TP} are separated by 20 Å (View 2), and the two Ile390 residues in β_E and β_{DP} are separated by 22 Å (View 3). It is clear from this illustration that the γ subunit must move in order to close β_E with simultaneous opening of β_{DP} or β_{TP} during catalysis.

The positions of Asp394 in the three β subunits and Ser83 in the γ subunit are also included in Fig. 1. The relative positions of these residues provide the structural basis for an experiment designed to identify the catalytic site in

the crystal structure corresponding to the high-affinity catalytic site that hydrolyzes substoichiometric ATP slowly in MF_1 and *E. coli* F_1 (Grubmeyer *et al*., 1982; Al-Shawi and Senior, 1988). According to the crystal structure, the side chain of γSer83 is within 7 Å of βAsp394 in β_{TP}, but is at 13 and 33 Å from the side chains of βAsp394 in β_{DP} and β_E, respectively. When a single catalytic site of the $\alpha_3(\beta D394C)_3(\gamma S83C)$ double-mutant subcomplex of TF_1 is loaded with Mg(2-N_3-[^{3}H]ADP), Mg(2-N_3-[^{3}H]ADP) plus $AlCl_3$ and NaF, or Mg(2-N_3-[^{3}H]ATP) followed by photolysis and then oxidation to cross link β to γ, in each case, none of the radioactivity was found in the β-γ cross-linked species (Dou, 1997). This suggests that in the absence of bound nucleotides, the catalytic sites display heterogeneous affinities for Mg-ADP or Mg-ATP dictated by the position of the asymmetrically arranged coiled-coil of the γ subunit. That no radioactivity was found in the cross-linked species suggests that β_{DP} and not β_{TP} in the crystal structure contribute to the high-affinity catalytic site identified under single-site conditions (Grubmeyer *et al*., 1982; Al-Shawi and Senior, 1988).

Figure 2A illustrates a minimal scheme that describes sequential opening and closing of the three catalytic sites of F_1 during ATP synthesis that is driven by clockwise rotation of the γ subunit through 360°. In each step, two β subunits are depicted in closed conformations (triangles) containing Mg-ATP bound to catalytic sites. The third β subunit is shown in an open conformation that is transiently empty and is awaiting energy-dependent binding of Mg-ADP and P_i, which has been observed in both oxidative and photosynthetic phosphorylation (Kayalar *et al*., 1976; Zhou and Boyer, 1993). It is postulated that low-affinity binding of Mg-ADP and P_i together to the open catalytic site triggers clockwise rotation of the γ subunit driven by ion translocation through F_o that forces closing of this catalytic site. In the top view in Fig. 2A, energy-dependent closing of catalytic site 3 is accompanied by synthesis of tightly bound Mg-ATP at this site and concerted opening of catalyic site 2 that allows dissociation of Mg-ATP synthesized two steps earlier. In this process, ion translocation drives clockwise rotation of the γ subunit by 120°. This model proposes that the transition state is formed as a catalytic site is converted from an open ground-state conformation to a closed ground-state conformation. Since ATP synthesis is postulated to occur during the closing process, the condensation of ADP with P_i is energy dependent. The ATP synthesized in this step remains tightly bound until it dissociates two steps later. The closed ground-state conformation of the catalytic site is thought to resemble the nearly common conformations of catalytic sites at the α_{DP}/β_{DP} and α_{TP}/β_{TP} in the crystal structure of MF_1, whereas the open ground-state conformation is thought to resemble that of the empty catalytic site at the α_E/β_E interface in the crystal structure.

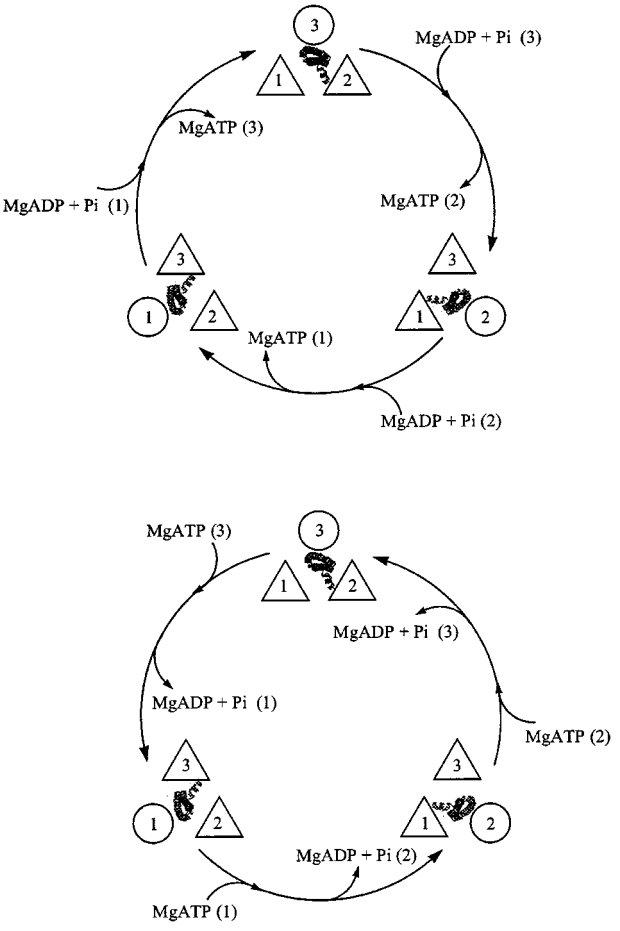

Fig. 2. Schemes for coupling rotation of the γ subunit to sequential opening of the three catalytic sites of F_1 during (A) ATP synthesis and (B) ATP hydrolysis under V_{max} conditions. Triangles represent β subunits in closed conformations containing Mg-ATP tightly bound to catalytic sites and circles represent β subunits that are transiently open with empty catalytic sites. The dotted lines between the triangles represent interaction of the side chains of Ile390 in adjacent, closed β subunits. The numbers, 1, 2, and 3 on the β subunits indicate the order in which catalytic sites of isolated F_1 are loaded with Mg-ADP or Mg-ATP under *in vitro* conditions (Dou, 1997). An abbreviated form of the γ subunit is shown in the center of each display of the three β subunits with the α-helical spur containing residue 73–90 pointing toward β_{TP}. The schemes are described in detail in the text.

Figure 2B illustrates a minimal scheme for sequential hydrolysis of ATP at three catalytic sites of either isolated F_1 or in F_oF_1 that drives rotation of the γ subunit through 360° in the counterclockwise direction. Again, in each step, two β subunits are depicted in closed conformations (triangles) containing Mg-ATP tightly bound to catalytic sites. The third β subunit is shown in the open

conformation with a transiently empty catalyic site that is awaiting binding of Mg-ATP for catalysis to continue. In the top view in Fig. 2B, closing of site 3 is initiated when Mg-ATP binds to it. This promotes opening of catalytic site 1 coupled to ATP hydrolysis, followed by dissociation of Mg-ADP and P_i. In this process, the concerted switching of site 1 from open to closed and site 2 from closed to the open drives rotation of the γ subunit through 120° in the counterclockwise direction. In F_oF_1, this rotation drives ion translocation through F_o.

According to these models, the transition state for ATP synthesis forms when a catalytic site switches from an open to a closed conformation and the transition state for ATP hydrolysis forms when a catalytic site switches from a closed to an open conformation. Therefore, the transition state is assumed to be formed when catalytic sites are in a hybrid conformation that lies between the nearly common ground-state conformation of the catalytic sites at the α_{TP}/β_{TP} and α_{DP}/β_{DP} interfaces in the x-ray structure, on the one hand, and the ground-state conformation of the catalytic site at the α_E/β_E interface on the other. It is also assumed that the hybrid conformation in which the transition state is formed, is the same during ATP synthesis and hydrolysis.

The models illustrated in Fig. 2 differ considerably from the binding change model for ATP synthesis and hydrolysis developed by Boyer (1993, 2000). The binding-change model assumes that V_{max} is attained when only two catalytic sites are saturated and that the transition state is formed when catalytic sites are in the closed conformation. Weber and Senior (1997) have proposed a variation of the binding-change model for ATP hydrolysis that accommodates earlier demonstration that V_{max} rates are attained when three catalytic sites are saturated (Weber *et al*., 1993). The proposed, three-site model suggests that during steady-state catalysis, two catalytic sites contain Mg-ADP and the third contains Mg-ATP. The model also assumes that the transition state is formed when a catalytic site is in the closed conformation. That two catalytic sites contain Mg-ADP and the third contains Mg-ATP under steady-state conditions is based on the different responses of the fluorescence spectrum of the βF155W mutant of *E. coli* F_1 on binding Mg-AMP–PNP or the Mg-ADP–fluoroberyllate, on the one hand, and Mg-ADP, on the other (Weber *et al*., 1996). In making these assignments, turnover-dependent entrapment of inhibitory Mg-ADP in catalytic sites was not taken into account nor was the fact that Mg-ADP–fluoroberyllate complexes are only formed in two catalytic sites (Issartel *et al*., 1991). The reliability of the βF155W mutant as a reporter of catalytic site occupancy during ATP hydrolysis became more suspect when it was subsequently reported that inhibition of ATP hydrolysis catalyzed by the βF155W mutant by azide is accompanied by entrapment of Mg-ATP in three catalytic sites (Weber and Senior, 1998). This contention conflicts with substantial evidence that has been accumulated indicating that azide inhibition is associated with entrapment of inhibitory Mg-ADP (Vasilyeva *et al*., 1982; Kalashnikova *et al*., 1988; Ren *et al*., 2000c). It is also inconsistent with the observation that hydrolysis of substoichiometric ATP by *E. coli* F_1 is not inhibited by azide (Noumi *et al*., 1987).

MUTATIONS THAT RELIEVE OR ENHANCE ENTRAPMENT OF INHIBITORY Mg-ADP

ATP hydrolysis by isolated F_1 or by the F_oF_1 complex is inhibited when Mg-ADP is entrapped in a single catalytic site. Entrapment can be accomplished by loading a single catalytic site with Mg-ADP or by loading a single catalytic site with Mg-ATP and allowing hydrolysis to occur (Drobinskaya *et al*., 1985; Milgrom and Murataliev, 1989; Chenyak and Cross, 1992; Jault and Allison, 1993; Dou *et al*., 1998). Transient, turnover-dependent entrapment of inhibitory Mg-ADP also occurs when isolated F_1-ATPases hydrolyze ATP in the absence of saturating noncatalytic sites with Mg-ATP (Vasilyeva *et al*., 1980; Milgrom *et al*., 1991; Jault and Allison, 1993; Jault *et al*., 1996). In the case of MF_1, binding Mg-PP_i to noncatalytic sites prevents entrapment of inhibitory Mg-ADP during turnover (Kalasnikova *et al*., 1988; Jault *et al*., 1994). Entrapment of inhibitory Mg-ADP is relieved when TF_1 hydrolyzes ATP in the presence of lauryl dimethylamine oxide (LDAO) (Paik *et al*., 1994).

Mutant forms of the $\alpha_3\beta_3\gamma$ subcomplex of TF_1 that have little or no propensity to entrap inhibitory Mg-ADP during turnover and resist inhibition by azide are thought to have increased stabilization of the open conformation of catalytic sites. Conversely, mutant forms that have increased propensity to entrap inhibitory Mg-ADP during turnover and increased sensitivity to inhibition by azide are thought to have increased stabilization of the closed conformation of catalytic sites. For instance, the $\alpha_3(\beta T163S)_3\gamma$ mutant subcomplex of TF_1 has little or no propensity to entrap Mg-ADP during turnover and is resistant to inhibition by azide, whereas the $\alpha_3(\beta E199C)_3\gamma$ subcomplex has increased propensity to entrap inhibitory Mg-ADP during turnover and increased sensitivity to inhibition by azide than the wild-type subcomplex. The wild-type TF_1 subcomplex has a K_m of 40 μM and a k_{cat} of 120 s^{-1} (Ren and Allison, 2000a), whereas the K_m and k_{cat} values of the βT163S mutant are 133 μM and 360 s^{-1}, respectively (Jault *et al*., 1996). In contrast, the K_m and K_{cat} values of the βE199C mutant are 1.6 μM and

6 s^{-1}, respectively, indicating that it has a much higher affinity for Mg-ATP. Comparison of fluorescence quenching of the $\alpha_3(\beta$E199C/Y345W$)_3\gamma$ double mutant and the $\alpha_3(\beta$Y345W$)_3\gamma$ single mutant by Mg-ATP is consistent with this conclusion. These comparisons suggest that the βThr163Ser substitution favors the open conformation of the catalytic site by decreasing direct interaction with the Mg^{2+} ion coordinated to bound nucleotides and/or by forming a stronger hydrogen bond with the carboxylate of βGlu199. They also infer that the βGlu199Cys substitution attenuates catalysis and increases affinity for ATP by preventing formation of a stable hydrogen bond with βThr163 when the catalytic site is empty (Ren and Allison, 2000a).

FORMATION OF INHIBITORY Mg-ADP–FLUOROALUMINATE COMPLEXES AT CATALYTIC SITES OF F_1

Formation of tightly bound Mg-ADP–fluoroaluminate complexes at catalytic sites of F_1 was first demonstrated by Lunardi *et al*. (1988) who found that incubation of MF_1 with excess ADP plus Mg^{2+}, $AlCl_3$, and NaF led to quasi-irreversible inactivation of ATP hydrolysis. It was subsequently reported by Issartel *et al*. (1991) that Mg-ADP–fluoroaluminate complexes are formed in two catalytic sites when $AlCl_3$ and NaF were added to MF_1 in the presence of excess ADP and Mg^{2+}.

Extending these studies, Dou *et al*. (1997) found that after loading Mg-ADP onto a single catalytic site of the $\alpha_3\beta_3\gamma$ subcomplex of TF_1 or a single catalytic site of nucleotide-depleted MF_1, ATP hydrolysis is slowly inactivated upon addition of Al^{3+} and F^-. In contrast, when Mg-ADP was loaded onto two catalytic sites of the enzymes or when the $\alpha_3\beta_3\gamma$ subcomplex of TF_1 was incubated with excess ADP plus Mg^{2+} before adding Al^{3+} and F^-, it was shown that inactivation occurs sixfold more rapidly. Therefore, positive catalytic to catalytic site cooperativity occurs when ADP–fluoroaluminate complexes are formed in two catalytic sites. It was also observed that the rate of formation of the Mg-ADP–fluoroaluminate complex is slowed considerably in the presence of P_i when Al^{3+} and F^- are added to F_1 after loading one or two catalytic sites with Mg-ADP. This suggests that binding of AlF_3 or AlF_4^- to a domain for P_i adjacent to bound Mg-ADP initiates an isomerization that leads to the tightly bound Mg-ADP–fluoraluminate complex. It has been reported that P_i binds to catalytic sites of MF_1 that contain bound Mg-ADP (Kozlov and Vulfson, 1985).

It was also observed that the rate of formation of Mg-ADP–fluoroaluminate complexes in two catalytic sites is accelerated further when the $\alpha_3\beta_3\gamma$ subcomplex of TF_1 is incubated with excess ADP plus Mg^{2+} and either P_i or sulfite before initiating inactivation by adding Al^{3+} and F^-. The observed acceleration under these conditions is thought to be caused by binding Mg-ADP and phosphate or sulfite together at noncatalytic sites and, therefore, represents noncatalytic to catalytic site cooperativity (Dou *et al*., 1997; Grodsky *et al*., 1998). Sulfite has been shown to accelerate formation of Mg-ADP–fluoroaluminate complexes at catalytic sites of MF_1 (Issartel *et al*., 1991).

Formation of cross links between the α and γ subunits and between the β and γ subunits by oxidation of the $(\alpha$A404C$)_3\beta_3(\gamma$S22C) and $\alpha_3(\beta$D394C$)_3(\gamma$S83C) mutant inactivates ATP hydrolysis and also abolishes cooperative formation of Mg-ADP–fluoroaluminate complexes in two catalytic sites. However, slow formation of the Mg-ADP–fluoroaluminate complex in a single catalytic site still occurs. The reduced subcomplexes exhibit cooperativity when Mg-ADP–fluoroaluminate complexes are formed at two catalytic sites (Dou *et al*., 1997). Similar loss of cooperativity is observed when the $\alpha_3(\beta$D315C/R337C$)_3\gamma$ and $\alpha_3(\beta$Y345W/I390C$)_3\gamma$ double mutants are converted to their oxidized forms (Ren *et al*., 1999; Ren and Allison, 2000c).

A possible explanation for the loss of cooperativity that occurs on cross linking the mutant enzymes is the following. It is reasonable to assume that loading Mg-ADP onto two catalytic sites of the wild-type or reduced-mutant subcomplexes, closes one site completely, whereas the other catalytic site only partly closes. Subsequent simultaneous binding of AlF_3 or AlF_4^- to both sites could induce closing coupled to isomerization at the partly closed site, which, in turn, promotes isomerization at the completely closed site. To explain loss of cooperativity in forming Mg-ADP–fluoroaluminate complexes when the mutant enzymes are oxidized, it is again reasonable to assume that cross linking prevents transmission of conformational signals from one catalytic site to the other. It has been shown that mutations in the α or β subunit that affect cooperativity of ATP hydrolysis either accelerate or attenuate cooperative formation of Mg-ADP–fluoroaluminate complexes (Dou *et al*., 1997; Grodsky *et al*., 1998). It is significant that the $(\alpha$D269N$)_3\beta_3\gamma$ subcomplex of TF_1 exhibits extremely slow formation of the Mg-ADP–fluoroaluminate complex when Mg-ADP is bound to a single catalytic site. This mutation is in the Walker B consensus sequence of α subunits and affects competent binding of nucleotides to noncatalytic sites (Jault *et al*., 1996). Therefore, the slow rate of formation of the Mg-ADP–fluoroaluminate complex observed with this mutant indicates that a catalytic site recognizes a defect in noncatalytic sites even when the latter sites are empty.

Based on differences in quenching of tryptophan fluorescence observed when the βTyr345Trp of *E. coli* F_1 was titrated with Mg-ADP in the presence and absence of Al^{3+} plus F^-, Nandanaciva *et al*. (1999a) reported that tightly bound Mg-ADP–fluoroaluminate complexes form in two catalytic sites of the enzyme. Using the same method of analysis, they also reported that Mg-ADP–fluoroaluminate complexes are not formed in catalytic sites of the βE188Q/Y345W, βK162Q/Y345W, αR373A/βY345W and αArg373Cys/βTyr345Trp double mutants of *E. coli* F_1 (Nandanaciva *et al.*, 1999b). Each double mutant contains an amino acid residue that interacts with anionic oxygens of ADP or AMP–PNP bound to catalytic sites in the crystal structure of MF_1 (see Table I). Since formation of Mg-ADP–fluoroaluminates was not observed in the double mutants, it was concluded that the Mg-ADP–fluoroaluminate complex detected at catalytic site 1 of the βTyr345Trp mutant represents a transition-state analog. Based on kinetic analysis of formation of Mg-ADP–fluoroaluminates in catalytic sites of nucleotide-depleted MF_1 and wild-type and mutant $\alpha_3\beta_3\gamma$ subcomplexes of TF_1, the validity of this conclusion is questionable (Dou *et al*., 1997; Grodsky *et al*., 1998; Ren *et al*., 1999).

It has been clearly shown that Mg-ADP–fluoroaluminate complexes are formed by binding AlF_3 or AlF_4^- to a catalytic site of nucleotide-depleted MF_1 or wild-type and mutant $\alpha_3\beta_3\gamma$ subcomplexes of TF_1 that already contains inhibitory Mg-ADP. This induces a slow isomerization that leads to formation of the more tightly bound Mg-ADP–fluoroaluminate complex (Dou *et al*., 1997). This means that a ground-state complex is converted to a more stable ground-state complex during the isomerization. It has also been shown that certain mutant forms of the $\alpha_3\beta_3\gamma$ subcomplex of TF_1 with defective ATPase activity form Mg-ADP–fluoroaluminate complexes in one or two catalytic sites at very reduced rates compared to wild type (Dou *et al*., 1997; Grodsky *et al*., 1998). Therefore, the relatively short time frame of the fluorescence measurements employed by Nandanaciva *et al*. (1999) may be responsible for their failure to detect formation of Mg-ADP–fluoroaluminates in certain double mutants of *E. coli* F_1 containing the βTyr345Trp substitution.

Recently, Braig *et al*. (2000) reported the X-ray structure deduced from crystals of MF_1 previously inactivated in the presence of excess Mg-ADP, $AlCl_3$, and NaF. The major difference between this crystal structure and the original X-ray structure (Abrahams *et al*., 1994) is the presence of electron density corresponding to planar AlF_3 at the catalytic site containing Mg-ADP at the α_{DP}/β_{DP} interface. Comparison of the two crystal structures indicates that only minor rearrangements of amino acid side chains occur when AlF_3 is entrapped in this catalytic site adjacent to bound Mg-ADP. From this comparison, the author conclude that the Mg-ADP–AlF_3 complex entrapped in the α_{DP}/β_{DP} catalytic site represents a transition-state analog and suggest that once nucleotide is bound to a catalytic site, only small changes are required to facilitate the hydrolytic reaction catalyzed by the enzyme. In contrast, we suggest that the comparison of the two crystal structures supports our contention that Mg-ADP–fluoroaluminate complexes tightly bound to catalytic sites of F_1 are ground-state analogs.

From the arguments presented in developing the schemes illustrated in Fig. 2, we contend that transition states are formed transiently in a hybrid conformation of the catalytic site when β subunits are in the process of closing during ATP synthesis or in the process of opening during ATP hydrolysis. To assure flawless rotation of the γ subunit, the common transition state for synthesis and hydrolysis must be of finite duration and formed with precise timing during sequential firing of catalytic sites.

ACKNOWLEDGMENT

This work was supported by U.S. Public Health Service Grant GM 16,974.

REFERENCES

Abrahams, J. P., Leslie, A. G. W., Lutter, R., and Walker, J. E. (1994). *Nature (London)* **370**, 621–628.
Allison, W. S. (1998). *Acc. Chem. Res.* **31**, 819–826.
Al-Shawi, M. K., and Senior, A. E. (1988). *J. Biol. Chem.* **263**, 19640–19648.
Boyer, P. D. (1993). *Biochim. Biophys. Acta* **1140**, 215–250.
Boyer, P. D. (2000). *Biochim. Biophys. Acta* **1458**, 252–262.
Braig, K., Menz, R. I., Montgomery, M. G., Leslie, A. G. W., and Walker, J. E. (2000). *Structure* **8**, 567–573.
Chernyak, B. V., and Cross, R. L. (1992). *Arch. Biochem. Biophys.* **295**, 247–252.
Dou, C. (1997). Ph. D. Dissertation, University of California at San Diego.
Dou, C., Grodsky, N. B., Matsui, T., Yoshida, M., and Allison, W. S. (1997). *Biochemistry* **36**, 3719–3727.
Dou, C., Fortes, P. A. G., and Allison, W. S. (1998). *Biochemistry* **37**, 16757–16764.
Duncan, T. M., Bulygin, V. V., Zhou, Y., Hutcheon, M. L., and Cross, R. L. (1995). *Proc. Natl. Acad. Sci. USA* **92**, 10964–10968.
Drobinskaya, I. Y., Kozlov, I. A., and Murataliev, M. B. (1985). *FEBS Lett.* **182**, 419–424.
Fillingame, R. H. (2000). *J. Exp. Biol.* **203**, 9–17.
Grodsky, N. B., Dou, C., and Allison, W. S. (1998). *Biochemistry* **37**, 1007–1014.
Groth, G. (2000). *Biochim. Biophys. Acta* **1458**, 417–427.
Grubmeyer, C., Cross, R. L., and Penefsky, H. S. (1982). *J. Biol. Chem.* **257**, 12092–12100.
Issartel, J. P., Dupuis, A., Lunardi, J., and Vignais, P. V. (1991). *Biochemistry* **30**, 4726–4753.

Jault, J.-M., and Allison, W. S. (1993). *J. Biol. Chem.* **269**, 319–325.
Jault, J.-M., Paik, S. R., Grodsky, N. B., and Allison, W. S. (1994). *Biochemistry* **33**, 1479–1485.
Jault, J.-M., Matsui, T., Jault, F. M., Kaibara, C., Muneyuki, E., Yoshida, M., Ohta, T., Kagawa, Y., and Allison, W. S. (1996). *J. Biol. Chem.* **271**, 28818–18824.
Kalashnikova, T, Y., Milgrom, Y. M., and Murataliev, M. B. (1988). *Eur. J. Biochem.* **177**, 213–218.
Kayalar, C., Rosing, J., and Boyer P. D. (1976). *Biochem. Biophys. Res. Comm.* **72**, 1153–1159.
Kozlov, I. A., and Vulfson, E. N. (1985). *FEBS Lett.* **182**, 425–428.
Lunardi, J., Dupuis, A., Garin, J., Issartel, J.-P., Michel, L., Chabre, M., and Vignais, P. V. (1988). *Proc. Natl. Acad. Sci. USA* **85**, 8958–8962.
Milgrom, Y. M., and Murataliev, M. B. (1989). *Biochim. Biophys. Acta*, **975**, 50–58.
Milgrom, Y. M., Ehler, L. L., and Boyer, P. D. (1991). *J. Biol. Chem.* **266**, 11551–11558.
Nandanaciva, S., Weber, J., and Senior, A. E. (1999a). *J. Biol. Chem.* **274**, 7052–7058.
Nandanaciva, S., Weber, J., Wilke-Mounts, S., and Senior, A. E. (1999b). *Biochemistry* **38**, 15493–15499.
Noji, H., Yasuda, R., Yoshida, M., and Konisita, K. (1997). *Nature (London)* **386**, 299–302.
Noumi, T., Maeda, M., and Futai, M. (1987). *FEBS Lett.* **213**, 381–384.
Omote, H., and Futai, M. (1998). *Acta Physiol. Scand.* **163**, 177–183.
Paik, S. R., Jault, J.-M., and Allison, W. S. (1994). *Biochemistry* **33**, 126–133.
Ren, H., and Allison, W. S. (2000a). *J. Biol. Chem.* **275**, 10057–10063.
Ren, H., and Allison, W. S. (2000b). *Biochim. Biophys. Acta* **1458**, 221–233
Ren, H., and Allison, W. S. (2000c). *J. Biol. Chem.*, submitted.
Ren, H., Dou, C., Stelzer, M. S., and Allison, W. S. (1999). *J. Biol. Chem.* **274**, 31366–31372.
Sabbert, D., Engelbrecht, S., and Junge, W. (1996). *Nature* **381**, 623–626.
Tsunoda, S. P., Muneyuki, E., Amano, T., Yoshida, M., and Noji, H. (1999). *J. Biol. Chem.* **274**, 5701–5706.
Vasileva, E. A., Fitin, A. F., Minkov, I. B., and Vinogradov, A. D. (1980). *Biochem. J.* **188**, 807–815.
Vasileva, E. A., Minkov, I. B., Fitin, A. F., and Vinogradov, A. D. (1982). *Biochem. J.* **202**, 15–23.
Weber, J., and Senior, A. E. (1997). *Biochim. Biophys. Acta* **1319**, 19–58.
Weber, J., and Senior, A. E. (1998). *J. Biol, Chem.* **273**, 33210–33215.
Weber, J., Wilke-Mounts, S., Lee, R. S. F., Grell, E., and Senior, A. E. (1993). *J. Biol. Chem.* **268**, 20126–20133.
Weber, J., Bowman, C., and Senior, A. E. (1996). *J. Biol. Chem.* **271**, 18711–18713.
Yasuda, R., Noji, H., Kinosota, K., and Yoshida, M. (1998). *Cell* **93**, 1117–1124.
Zhou, J.-M., and Boyer, P. D. (1993). *J. Biol. Chem.* **268**, 1531–1538.